


Lyapunov spectra and collective modes of chimera states in globally coupled Stuart-Landau oscillators

Kevin Höhlein, Felix P. Kemeth, and Katharina Krischer 

Physik-Department, Nonequilibrium Chemical Physics, Technische Universität München, D-85748 Garching, Germany



(Received 17 April 2019; published 20 August 2019)

Oscillatory systems with long-range or global coupling offer promising insight into the interplay between high-dimensional (or microscopic) chaotic motion and collective interaction patterns. Within this paper, we use Lyapunov analysis to investigate whether chimera states in globally coupled Stuart-Landau (SL) oscillators exhibit collective degrees of freedom. We compare two types of chimera states, which emerge in SL ensembles with linear and nonlinear global coupling, respectively, the latter introducing a constraint that conserves the oscillation of the mean. Lyapunov spectra reveal that for both chimera states the Lyapunov exponents split into several groups with different convergence properties in the limit of large system size. Furthermore, in both cases the Lyapunov dimension is found to scale extensively and the localization properties of covariant Lyapunov vectors manifest the presence of collective Lyapunov modes. Here, however, we find qualitative differences between the two types of chimera states: Whereas the ones in the system under nonlinear global coupling exhibit only slow collective modes corresponding to Lyapunov exponents equal or close to zero, those which experience the linear mean-field coupling exhibit also faster collective modes associated with Lyapunov exponents with large positive or negative values. Furthermore, for the fastest collective mode we showed that it spreads across both synchronous and incoherent oscillators.

DOI: [10.1103/PhysRevE.100.022217](https://doi.org/10.1103/PhysRevE.100.022217)

I. INTRODUCTION

Chaos readily emerges in systems composed of many coupled oscillatory “units.” These units may represent individual oscillators or infinitesimally small patches of spatially extended oscillatory media, and the coupling is what gives rise to chaotic instabilities. The origin of the instabilities, however, might lie in microscopic (i.e., local) interactions, involving only a small number of oscillators or may result from complex interaction patterns on macroscopic system scales. The character of the corresponding chaotic dynamics, accordingly, may vary significantly.

One way to shine light on the nature of the chaotic dynamics is to study chaotic states in oscillatory ensembles containing different numbers of oscillators N while being subject to equivalent coupling schemes. Thereby, the chaotic dynamics are usually characterized in terms of Lyapunov exponents (LEs), which measure the average infinitesimal divergence rates of the motion in phase space [1,2]. Our understanding of chaos within this context is comparatively advanced in two limiting cases, so-called intensive and solely extensive chaos. Intensive chaos is characterized by an (in general small) number of positive LEs that is independent of the number of oscillatory units. It occurs, e.g., for certain parameters in systems of globally coupled oscillators [3–5]. In the opposite case, when the chaotic motion arises exclusively from microscopic degrees of freedom and the number of positive LEs scales linearly with N , then the chaotic dynamics is solely extensive. Such behavior was shown to exist in some generic spatially one-dimensional models [6]. However, it has been recently established that large systems with global coupling schemes or spatially extended systems in two or

three spatial dimensions, might exhibit chaotic motion that belongs to neither of these two situations. Instead, their dynamics are characterized by both a few collective macroscopic modes and a large number of microscopic, chaotic degrees of freedom [3–5]. Our knowledge how and when such collective modes develop and which role they play in the overall high-dimensional chaotic dynamics is still very limited.

The investigation of collective dynamics in high-dimensional chaotic systems remains a challenge. For a long time, it was common belief that conventional Lyapunov analysis cannot capture these collectively chaotic dynamics correctly [7]. Instead, finite-size perturbations needed to be studied in order to identify collective dynamical modes and the associated LEs. Only recently, Takeuchi *et al.* [8,9] were able to demonstrate that standard Lyapunov analysis can in fact provide information on collective dynamics. The key of their analysis was the calculation of the covariant Lyapunov vectors (CLVs) associated with the LEs [1,10,11]. Having access to CLVs, Takeuchi *et al.* complemented the information provided by the Lyapunov spectrum with an investigation of the localization or delocalization properties of CLVs associated with particular LEs. They illustrated their strategy for N globally coupled Stuart-Landau (SL) oscillators in a high-dimensional chaotic state. Most of the CLVs were found to be well localized for a large range of ensemble sizes N , while a small number of modes appeared to become increasingly delocalized with increasing N . The respective perturbations, named collective Lyapunov modes, were shown to be related to macroscopically chaotic degrees of freedom. Moreover, in accordance with earlier work on collective chaos by Nakagawa and Kuramoto [5,12,13], they showed that the overall Lyapunov spectrum can be separated into parts with

different convergence properties in the limit of large N . In particular, they identified an extensively scaling group of $\mathcal{O}(N)$ positive LEs in the middle of the spectrum, resulting in a flattening of the spectrum. Around the most positive and most negative exponents, however, they also observed subextensive groups of exponents, the number of which was shown to scale approximately as $\mathcal{O}[\ln(N)]$ [9]. In other studies, the localization properties of CLVs were elaborated. In scale-free networks of chaotic maps Kuptsov and Kuptsova [14] observed a localization of nodes which were preserved in the course of the dynamics. Xu and Paul [15] studied CLVs in Rayleigh-Bénard convection and could correlate spatial localization of the CLVs with defect structures in the fluid flow field.

In this paper, we perform a related Lyapunov analysis of chimera states in globally coupled SL oscillators. Being composed of coexisting groups exhibiting synchronous and asynchronous motion, respectively, chimera states are peculiar dynamic states which can be seen as “a natural link between coherence and incoherence” [16]. They might offer insight into natural phenomena such as some neural activity patterns [17] or hydrodynamic flows with mixed laminar and turbulent patterns [18]. So far, there are only a few studies on Lyapunov analysis of chimera states that mainly focus on systems of coupled phase oscillators. Wolfrum *et al.* [19,20] showed that the Lyapunov spectra for chimera states in coupled phase oscillator networks of finite size exhibit an extensive number of positive LEs, revealing the hyperchaotic nature of chimera states. Yet, all the positive exponents decay with increasing system size and finally yield neutrally stable zero exponents in the limit $N \rightarrow \infty$. Nevertheless, they found the Lyapunov dimension D_L to scale extensively with system size. Furthermore, Botha *et al.* [21,22] studied the distribution of finite-time LEs in chimera-like dynamics and identified characteristic patterns in their temporal distribution function. While for usual chaotic states without synchronization pattern the finite-time LEs follow a Gaussian distribution, they found that the distribution in the case of chimera states possesses a complex, multimodal shape, which they proposed to use as an indicator for chimera-like behavior.

In this work, however, we want to focus our attention on properties of the asymptotic Lyapunov spectra, without further reference to the temporal distribution of finite-time exponents. In particular, we examine whether Lyapunov spectra for chimera states of the globally coupled SL ensemble exhibit similar patterns as observed for the above-mentioned chaotic states, which exist in the same type of oscillatory network for different parameter values [8]. Furthermore, we compare chimera states in these mean-field coupled SL ensembles with those arising in SL oscillators subject to a nonlinear global coupling that conserves a harmonic oscillation of the ensemble mean. This coupling scheme was introduced to describe experiments on Si electrodisolution [23,24]. In our context, it gives additional information of how a global constraint might further impact the interplay between high-dimensional incoherent motion and collective interaction patterns.

The paper is organized as follows. In the next section, we introduce our two models as well as the particular types of chimera states that are subject to our investigations. In Sec. III, the notation used throughout the paper is introduced,

Lyapunov analysis as performed on our data reviewed, and measures used to characterize the dynamics, in particular the Lyapunov dimension D_L and the inverse participation ratio (IPR) as well as a group localization index ρ_x , are defined. In the results and discussion Sec. IV, we start by investigating the Lyapunov spectra of the two types of chimera states for $N = 16$ oscillators in detail, discuss then how the spectra change when N is stepwise doubled up to $N = 256$, and end with a discussion of how the Lyapunov dimension and the IPR depend on N . The latter allows us in particular to draw conclusion on the existence and on some properties of collective Lyapunov modes. The paper is completed with the conclusion Sec. V.

II. DYNAMICAL SYSTEMS

There is a vast number of different chimera states that have been reported in the literature in recent years [25–28]. In this article, we focus on two kinds, also called type I and type II chimeras [29], which can be observed in systems with long-range interactions [23,30]. The former, the type I chimera, appears in Stuart-Landau ensembles with linear global coupling. The time evolution of the systems is governed by equations of the form

$$\partial_t W_k = W_k - (1 + ic_2)|W_k|^2 W_k + \kappa \left(\frac{1}{N} \sum_{j=1}^N W_j - W_k \right), \quad (1)$$

wherein W_k denotes the complex amplitude of oscillator k , and $k = 1, \dots, N$, with N being the total number of oscillators. Parameters are the real shear, c_2 , and the complex coupling constant, κ , which we set to $c_2 = 2$ and $\kappa = 0.7(1 - i)$ in the following. Hereby i denotes the imaginary unit. Given this set of parameters, we investigate ensemble sizes $N = 2^l$ for $4 \leq l \leq 8$ and find the type I chimera state to be a stable attractor for $N \geq 16$. The oscillator dynamics in the complex plane, as well as the corresponding time series of the real parts are shown in Figs. 1(a) and 1(c), respectively, for $N = 256$. There one observes a coherent group of oscillators, depicted in dark red (dark gray), with a larger absolute value of W_k , and an incoherent group composed of oscillators with smaller amplitudes, shown in orange (light gray). The thick dots highlight a snapshot of the dynamics. Note that the motion of the incoherent group, when viewed in the complex plane, lies on a stringlike object undergoing stretching and folding. The structure is similar to a Birkhoff-Shaw attractor [31] and resembles the chaotic motion found in mean-field coupled SL ensembles [8,12].

In contrast to the type I chimeras, the type II chimera state has only been observed in systems with nonlinear global coupling [29]. In particular, it appears in Stuart-Landau ensembles of the form

$$\partial_t W_k = -ivW_k - (1 + iv) \left(\frac{1}{N} \sum_{j=1}^N W_j - W_k \right) - (1 + ic_2) \left(\frac{1}{N} \sum_{j=1}^N |W_j|^2 W_j - |W_k|^2 W_k \right), \quad (2)$$

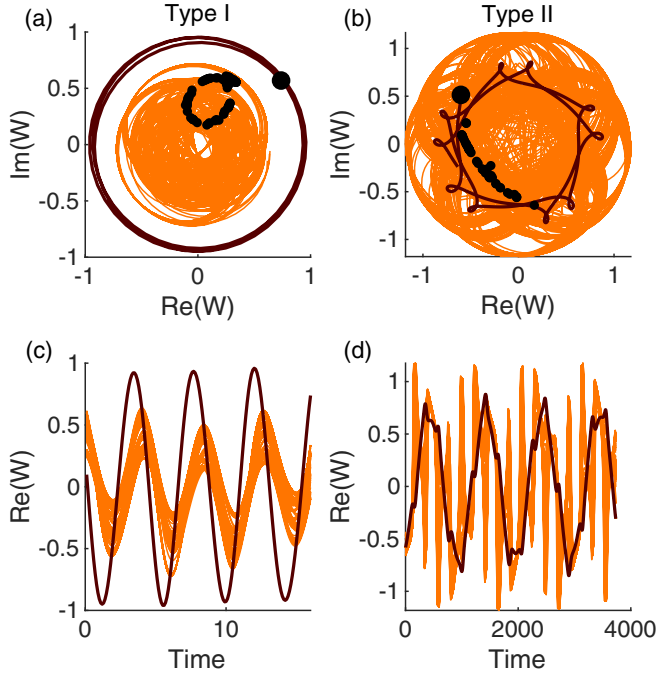


FIG. 1. Simulation data of the type I chimera, (a) and (c), and the type II chimera state, (b) and (d), with $N = 256$ oscillators. Trajectories of coherent and incoherent oscillators are shown in dark red (dark gray) and orange (light gray), respectively. Top: Oscillator trajectories in the complex plane. Dots represent a snapshot of the oscillator states. Bottom: Real part of the oscillator states as a function of time.

in certain regions of parameter space. Exemplary simulation data with parameters $c_2 = -0.66$, $\nu = 0.1$ and the initial absolute value of the mean amplitude,

$$|\langle W \rangle| = \left| \sum_j W_k(t=0)/N \right| = \eta = 0.67,$$

are depicted in Figs. 1(b) and 1(d) for $N = 256$. The coloring scheme is identical to that of the type I chimera state. Note that the type II chimera state exhibits an additional frequency component in the oscillator dynamics and that there is no clear amplitude separation between the coherent and incoherent oscillators, as opposed to the type I dynamics. Furthermore, qualitative differences between both types of chimera states can be captured in terms of order parameters [26]: While the type II chimera states possess an order parameter with oscillatory behavior, leading to a categorization as “breathing chimeras,” the order parameter of the type I chimera state fluctuates irregularly around a constant value, as characteristic for the class of “turbulent chimeras.” In the following, we investigate the ensemble dynamics of the two cases more carefully using Lyapunov analysis, with a particular emphasis on the apparently chaotic motion of the oscillators in the incoherent groups.

III. BACKGROUND AND METHODS

A. Lyapunov analysis

Lyapunov analysis provides quantitative methods to investigate the degree of chaoticity of dynamical systems [2]. To introduce concepts and notation, we consider a sufficiently well-behaved dynamical system, whose time evolution is described by a time-dependent vector $\mathbf{x} = \mathbf{x}(t) \in \mathbb{R}^{2N}$ and governed by the autonomous ordinary differential equation

$$\dot{\mathbf{x}} = \mathbf{f}(\mathbf{x}). \quad (3)$$

Equations (1) and (2) can be cast in this form by introducing the real-valued oscillator coordinates $\{a_k, b_k\}_{k=1}^N$ through

$$a_k = \frac{1}{\sqrt{2}}(W_k + W_k^*),$$

$$b_k = -\frac{i}{\sqrt{2}}(W_k - W_k^*),$$

wherein W_k^* denotes the complex conjugate of W_k . Organizing all coordinates in a $2N$ -dimensional state vector then yields

$$\mathbf{x} = \begin{pmatrix} \mathbf{a} \\ \mathbf{b} \end{pmatrix} = (a_1, \dots, a_N, b_1, \dots, b_N)^T.$$

Furthermore, we specify a reference trajectory $\hat{\mathbf{x}}(t)$, which at any point in time has to satisfy Eq. (3) and investigate the growth or decay of small perturbations around $\hat{\mathbf{x}}(t)$. The time evolution of infinitesimal perturbations $\delta\mathbf{x} = \delta\mathbf{x}(t) \in T_{\hat{\mathbf{x}}(t)}\mathbb{R}^{2N}$ is governed by the tangent-space dynamics

$$\delta\dot{\mathbf{x}} = \left. \frac{\partial \mathbf{f}}{\partial \mathbf{x}} \right|_{\hat{\mathbf{x}}(t)} \delta\mathbf{x}, \quad (4)$$

wherein $\left. \frac{\partial \mathbf{f}}{\partial \mathbf{x}} \right|_{\hat{\mathbf{x}}(t)}$ is the Jacobian matrix of $\mathbf{f}(\mathbf{x})$, evaluated at $\hat{\mathbf{x}}(t)$, and $T_{\hat{\mathbf{x}}(t)}\mathbb{R}^{2N}$ denotes the tangent space of the dynamical system in the vicinity of $\hat{\mathbf{x}}(t)$. For our purposes, we have $T_{\hat{\mathbf{x}}(t)}\mathbb{R}^{2N} \cong \mathbb{R}^{2N}$.

Given a suitable initial condition $\delta\mathbf{x}(t_0) = \delta\mathbf{x}_0 \in \mathbb{R}^{2N}$, Eq. (4) possesses the formal solution

$$\delta\mathbf{x}(t) = \Psi_{\hat{\mathbf{x}}}(t, t_0)\delta\mathbf{x}_0, \quad (5)$$

wherein $\Psi_{\hat{\mathbf{x}}}(t, t_0)$ denotes the fundamental matrix of Eq. (4), encoding the time evolution of perturbation vectors from $T_{\hat{\mathbf{x}}(t_0)}\mathbb{R}^{2N}$ at time t_0 to $T_{\hat{\mathbf{x}}(t)}\mathbb{R}^{2N}$ at time t . Using Eq. (5), as well as the standard scalar product in \mathbb{R}^m , the squared amplitude of some perturbation vector $\delta\mathbf{x}(t)$ can thus be expressed as

$$\|\delta\mathbf{x}(t)\|^2 = \delta\mathbf{x}_0^T \Psi_{\hat{\mathbf{x}}}(t, t_0)^T \Psi_{\hat{\mathbf{x}}}(t, t_0) \delta\mathbf{x}_0.$$

Oseledets’ theorem, also known as the multiplicative ergodic theorem [1], states that under rather general conditions there exist symmetric matrices

$$M_{\hat{\mathbf{x}}(t_0)}^{(\pm)} = \lim_{t \rightarrow \pm\infty} [\Psi_{\hat{\mathbf{x}}}(t, t_0)^T \Psi_{\hat{\mathbf{x}}}(t, t_0)]^{\frac{1}{2t}}, \quad (6)$$

with real positive eigenvalues $\mu_1 > \mu_2 > \dots > \mu_r$, $r \leq 2N$, which thus characterize the long-term expansion and contraction rates of perturbation vectors. In what follows, we will refer to the eigenspaces of $M_{\hat{\mathbf{x}}(t_0)}^{(\pm)}$ associated with eigenvalue μ_k as $U_{\hat{\mathbf{x}}(t_0), k}^{(\pm)}$. Note here that symmetries of the system as well as of the dynamical pattern can give rise to degeneracies in the spectrum, which we will discuss later on in more detail.

Denoting with g_k the degree of degeneracy of eigenvalue μ_k , the degeneracies satisfy $\sum_{k=1}^r g_k = 2N$ and agree with the dimensionality of the corresponding eigenspaces $U_{\hat{x}(t_0),k}^{(\pm)}$. Furthermore, the eigenvalues μ_k and degrees of degeneracy g_k coincide for $M_{\hat{x}(t_0)}^{(+)}$ and $M_{\hat{x}(t_0)}^{(-)}$ and are independent of the particular reference trajectory for ergodic dynamics. The Lyapunov exponents $\lambda_1 > \lambda_2 > \dots > \lambda_r$ are then defined through $\lambda_k = \ln \mu_k$ and satisfy

$$\|\Psi_{\hat{x}}(t, t_0)\delta\mathbf{x}_0\| \sim e^{\lambda_k t} \|\delta\mathbf{x}_0\| \quad (7)$$

for $\delta\mathbf{x}_0 \in \Omega_{\hat{x}(t_0),l}$. Therein, the subspaces $\Omega_{\hat{x}(t_0)}^{(k)} \subset T_{\hat{x}(t_0)}\mathbb{R}^{2N}$ are defined as follows: Employing the above notation, we set

$$\Gamma_{\hat{x}(t_0),k}^{(+)} = \bigoplus_{l=k}^r U_{\hat{x}(t_0),l}^{(+)},$$

$$\Gamma_{\hat{x}(t_0),k}^{(-)} = \bigoplus_{l=1}^k U_{\hat{x}(t_0),l}^{(-)},$$

with \bigoplus denoting the direct sum of vector spaces, and obtain

$$\Omega_{\hat{x}(t_0),k} = \Gamma_{\hat{x}(t_0),k}^{(+)} \cap \Gamma_{\hat{x}(t_0),k}^{(-)}.$$

The set of subspaces $\{\Omega_{\hat{x}(t_0),k} : 1 \leq k \leq r\}$ is called Oseledets' splitting [1,10] and provides a nonorthogonal decomposition of the tangent space according to different expansion rates of infinitesimal perturbations, i.e.,

$$T_{\hat{x}(t_0)}\mathbb{R}^{2N} = \bigoplus_{k=1}^r \Omega_{\hat{x}(t_0),k}.$$

The Oseledets subspaces satisfy $\dim(\Omega_{\hat{x}(t_0),k}) = g_k$. In contrast to the eigenspaces $U_{\hat{x}(t_0),l}^{(\pm)}$ of $M_{\hat{x}(t_0)}^{(\pm)}$, Oseledets' splitting is norm independent, invariant under time inversion, and depends on the current system state in a way that is covariant with respect to the dynamical flow, i.e.,

$$\Omega_{\hat{x}(t),k} = \Psi_{\hat{x}}(t, t_0)\Omega_{\hat{x}(t_0),k}.$$

The spanning vectors of Oseledets' splitting are called CLVs [10,32,33] and by virtue of Eq. (7) indicate the local orientation of stable and unstable manifolds in phase space. The spanning vectors of the orthogonal eigenspaces of $M_{\hat{x}(t_0)}^{(\pm)}$ are known as forward [FOLVs, (+)] and backward orthogonal Lyapunov vectors [BOLVs, (-)]. Despite the superior dynamical properties of CLVs compared to FOLVs and BOLVs, the efficient computation of CLVs has become possible only recently due to algorithms by Ginelli *et al.* [10], Wolfe and Samelson [11], and later on Kuptsov and Parlitz [32], who improved on the method by Wolfe and Samelson. CLVs have since attracted much scientific interest and proved to be a fruitful source of insight, especially into phase-space structures of high-dimensional dynamical systems. In particular, CLVs have been used to study, e.g., dynamics of rigid disk systems [34,35], chaotic motion in spatially extended systems [36,37], stability properties of geophysical models [38], and collective chaos in systems of coupled oscillators [8,9,39].

B. Lyapunov dimension and inverse participation ratio

The dimensionality of a chaotic attractor can be estimated from the Lyapunov dimension

$$D_L := L + \frac{\sum_{l=1}^L \lambda_l}{|\lambda_{L+1}|}. \quad (8)$$

with $L \leq 2N$ denoting the largest integer for which $\sum_{l=1}^L \lambda_l > 0$. Note here that for computing D_L , we have to take account for degeneracies in the Lyapunov spectrum explicitly. The summation in Eq. (8) therefore runs over an extended index $l \in \{1, \dots, 2N\}$, which enumerates all of the $2N$ potentially degenerate LEs in a way that satisfies $\lambda_1 \geq \lambda_2 \geq \dots \geq \lambda_{2N}$. Under generic circumstances, the Kaplan-Yorke conjecture then states that D_L is an upper bound of the information dimension D_1 of the dynamical pattern [40], which is obtained as a special case of the Renyi- q dimension for $q = 1$ [41,42] and is closely related to the information production in the underlying system [43]. A linear scaling of D_L with the system size, i.e., in our case the number of oscillators N , is commonly used to demonstrate extensivity of chaotic dynamics.

As mentioned above, oscillatory systems with global coupling schemes might also possess collective modes arising from strong correlations [3–5], which do not scale linearly with system size. Such collective modes can be identified investigating the localization or delocalization properties of CLVs associated with particular LEs. Using oscillator coordinates and the above notation, an arbitrary perturbation can be expressed as

$$\delta\mathbf{x} = (\delta a_1, \dots, \delta a_N, \delta b_1, \dots, \delta b_N)^T \in \mathbb{R}^{2N}, \quad (9)$$

wherein δa_k and δb_k denote the relative perturbation amplitudes affecting the real and imaginary part of the oscillator state W_k , respectively. As demonstrated by Takeuchi *et al.* [8], the inverse participation ratio (IPR) defined by Mirlin *et al.* [44] is a suitable measure for vector localization. For perturbations in the form of Eq. (9), the IPR can be written as

$$\text{IPR} = \sum_{k=1}^N (\delta a_k^2 + \delta b_k^2)^2. \quad (10)$$

Therein, we assume vector normalization according to $\sum_{k=1}^N (\delta a_k^2 + \delta b_k^2) = 1$. By definition, the IPR then takes values between N^{-1} and 1. Large values are obtained if the vector under study possesses a small number of large-amplitude components, indicating localization of the perturbation mode. Smaller values are obtained if all terms in the summation are of similar magnitude so that a greater number of oscillators is affected by the perturbation. A small IPR value is thus indicative of a collective Lyapunov mode.

For chimera states it is of particular interest whether the perturbations spread across synchronized and incoherent groups or whether they remain localized within one of the two groups. Since the IPR does not allow for a discrimination of intra- and intergroup delocalizations, we define a group localization index ρ_x according to

$$\rho_x = \frac{\text{IPR}_x / \text{IPR}}{N_x / N} \quad (11)$$

with

$$\text{IPR}_x = \sum_{k=1}^{N_x} (\delta a_k^2 + \delta b_k^2)^2. \quad (12)$$

Here, x refers to “sync” or “inc,” N_x being thus either the number of synchronized or the number of incoherent oscillators. IPR_x measures the share of the two groups in the total IPR and ρ_x scales it to the respective normalized group size. Consequently, if the group localization index $\rho_x = 1$, then $\rho_{\text{sync}} = \rho_{\text{inc}}$ and the mean perturbation of oscillators in both groups is equal, i.e., the intergroup delocalization is maximum. If, on the other hand, $\rho_{\text{inc}} > 1 (< 1)$, then the perturbations are more localized on the incoherent (synchronized) group.

C. Numerical methods and simulation details

For the integration of the system dynamics, we use the variable-step Dormand-Prince method [45] implemented in the explicit Matlab integration function ode45 [46] with a maximum time step of 5×10^{-3} for Eq. (1) and 1.5×10^{-2} for Eq. (2). During simulation of the type I chimera states, we allowed an initialization period of at least $10\,000N$ periods of the dynamics for the system state to settle down to an attractor. In the case of type II chimera states, we observe extremely long oscillatory transients, during which the number of synchronized oscillators increases with time. The duration of the transients is found to scale exponentially with system size and is of the order of 10^6 periods of the dynamics for $N = 256$. For a give system size, we find that the time between successive oscillators joining the synchronized cluster grows exponentially with increasing size of the cluster. The observed dynamics might be related to supertransients as reported in Ref. [19], but a more detailed analysis of the transients is beyond the scope of this paper. In order to minimize the influence of transient dynamics on our studies, we chose the initialization period so long as to observe no more changes in the number of synchronized oscillators for at least $10\,000N$ periods. Based on an analysis of Fourier spectra, we assume average period lengths of the dynamics of approximately 4.2 time units for type I and 12.9 for type II chimera states, independent of the system size N . For the computation of LEs and BOLVs, we employ the standard method developed independently by Shimada *et al.* [47] and Benettin *et al.* [48] and reviewed by Eckman *et al.* [49]. It is based on repeatedly performing QR decompositions and averaging over the logarithmic diagonal

entries of the R matrices for a sufficiently long time. We choose to perform 20 QR decompositions per period of the dynamics. Expecting an exponential convergence of the Q matrices containing the BOLVs, we admit a transient period of at least $1000N$ periods before recording the LEs and BOLVs. The CLVs are obtained from the BOLVs and the respective R matrices by applying the dynamic algorithm by Ginelli *et al.* [10]. In backward-time direction, we admit an initialization period of at least $100N$ periods before recording the CLVs. The final estimate of the LEs is obtained from an average over at least 2.5×10^4 periods of the dynamics. The CLVs are saved after each QR -step (resulting in 20 samples per period) over a time interval of 2.5×10^4 periods. Based on the statistics of the short-time estimates, we expect an accuracy of the exponents of at least 10^{-3} .

IV. RESULTS AND DISCUSSION

A. Lyapunov spectra for $N = 16$ oscillators

Figure 2 shows Lyapunov spectra of the type I and type II chimera states for a system size of $N = 16$ oscillators. Simplifying further discussions, we plot the full spectra, consisting of $2N = 32$ exponents, without removing degenerate exponents. We furthermore follow the suggestion of Ref. [2] and introduce the rescaled index

$$\tilde{l} := (l - 1/2)/(2N) \in (0, 1),$$

which enables us to show spectra for different ensemble sizes over the same abscissa range. The simulation data, used to generate the spectra, is not depicted here but resembles the data in Fig. 1 closely. For the type I dynamics, we find a group of $N_{\text{sync}} = 10$ synchronized oscillators, which coexists with $N_{\text{inc}} = 6$ oscillators performing incoherent motion. For the type II dynamics, the fraction of synchronized oscillators is higher with $N_{\text{sync}} = 13$ and $N_{\text{inc}} = 3$. The clustering of the oscillators into synchronized and incoherent groups induces a similar grouping pattern also for the LEs: These can be assigned to four main groups—P, N, and $\text{Cl}_{1,2}$ —which are separated by a small number of singleton exponents: Z and $\text{S}_{1,2}$.

Starting with P, the group of positive exponents, we recognize that both types of chimera states possess $N_{\text{inc}} - 1$ positive exponent, revealing their hyperchaotic character. In addition to P, we find a group N of negative exponents, with the same number of exponents, cf. Fig. 2. The facts that P and N are

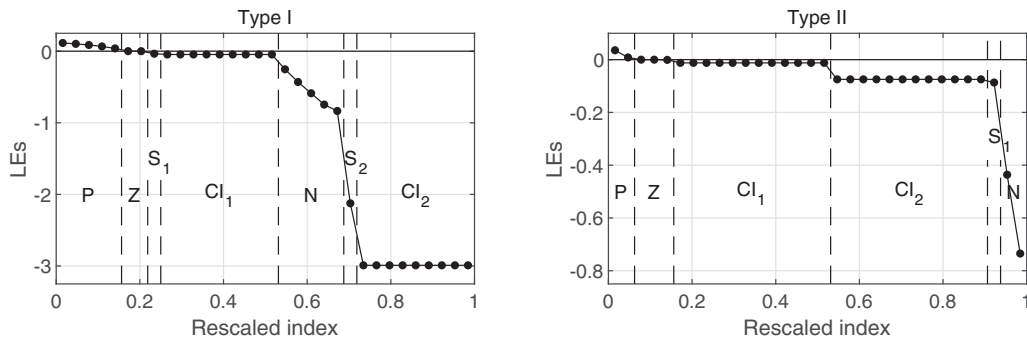


FIG. 2. Lyapunov spectra of a type I chimera state in Eq. (1) and a type II chimera state in Eq. (2) for a system size of $N = 16$ oscillators.

identical in size, and that the number of exponents appears to relate to the number of incoherent oscillators in the ensemble, suggests that P and N exponents correspond to stable and unstable directions in tangent space, which affect the group of incoherent oscillators predominantly. As we discuss in Sec. IV D in more detail, the shapes of the corresponding CLVs support this finding: All CLVs associated with the P and N exponents perturb all synchronized oscillators in the same way, without disturbing the clustering pattern.

Besides groups P and N, we find a group Z of very small exponents with values of the order of 10^{-4} or smaller. We observe two such exponents for the type I chimera state and three for the type II dynamics. These numbers are consistent with the number of zero exponents to be expected from symmetry considerations of Eqs. (1) and (2). The governing laws of both systems are independent of time, so that for any solution $\hat{W}(t)$ of Eqs. (1) or (2) the time-shifted solution $\hat{W}(t + \delta t)$ provides a valid trajectory, as well. Perturbations along the dynamical flow therefore neither grow nor decay in time, resulting in a neutrally stable direction of perturbation and a zero LE. Trivially, the invariance is preserved also when changing to the real-valued coordinates. With Eq. (3) it is easy to see that the corresponding CLV is

$$\delta \mathbf{x}_{\text{ts}} \propto \mathbf{f}[\hat{\mathbf{x}}(t)],$$

which, by chain rule, satisfies Eq. (4). Similarly, Eqs. (1) and (2) are invariant with respect to phase shifts in the complex plane, i.e., for any angle $\phi \in \mathbb{R}$, $e^{i\phi} \hat{W}(t)$ is a valid solution if the same is true for $\hat{W}(t)$. As a result, another zero exponent is associated with the covariant Lyapunov vector

$$\delta \mathbf{x}_{\text{ps}} \propto (-b_1, \dots, -b_N, a_1, \dots, a_N)^T,$$

corresponding to an infinitesimal rotation of all oscillators in the complex plane.

For the type II chimera state in Eq. (2), we have an additional zero exponent, which arises from the conservation law

$$d/dt |\langle W \rangle| = 0. \quad (13)$$

This can be seen from the fact that

$$d\langle W \rangle/dt = -iv\langle W \rangle, \quad (14)$$

wherein $\langle W \rangle = \sum_{k=1}^N W_k/N$ denotes the complex amplitude of the mean field. According to Eq. (14), $\langle W \rangle$ performs a harmonic oscillation in time and thus conserves the mean-field amplitude. The conservation law (13) induces a splitting of phase space into invariant manifolds associated with different values of $|\langle W \rangle| = \eta$ and thus yields another neutrally stable direction in tangent space. The CLV associated with this direction, however, appears to possess a nontrivial structure so that an analytical expression has not been identified, yet.

Two further groups of exponents, $\text{CI}_{1,2}$, are made up of only two distinct LEs, possessing a $(N_{\text{sync}} - 1)$ -fold degeneracy each. Clearly, these degeneracies originate from the synchronization pattern of the chimera states. To see this, we take a closer look on the tangent space dynamics in presence of synchronized oscillators. Extending the notation of Eq. (3),

we write

$$\dot{\mathbf{x}} = \begin{pmatrix} \dot{\mathbf{a}} \\ \dot{\mathbf{b}} \end{pmatrix} = \begin{bmatrix} \mathbf{f}^{(a)}(\mathbf{a}, \mathbf{b}) \\ \mathbf{f}^{(b)}(\mathbf{a}, \mathbf{b}) \end{bmatrix} = \mathbf{f}(\mathbf{x}),$$

with $\mathbf{a} = (a_1, \dots, a_N)^T$ and $\mathbf{b} = (b_1, \dots, b_N)^T$. The Jacobian matrix of the overall system can then be written in block-matrix form as

$$\frac{\partial \mathbf{f}}{\partial \mathbf{x}} = \begin{bmatrix} \frac{\partial \mathbf{f}^{(a)}}{\partial \mathbf{a}} & \frac{\partial \mathbf{f}^{(a)}}{\partial \mathbf{b}} \\ \frac{\partial \mathbf{f}^{(b)}}{\partial \mathbf{a}} & \frac{\partial \mathbf{f}^{(b)}}{\partial \mathbf{b}} \end{bmatrix}. \quad (15)$$

Denoting the k th coordinate of $\mathbf{f}^{(a)}$ with $f_k^{(a)}$, the global coupling scheme in Eqs. (1) and (2) allows us to separate the terms according to

$$f_k^{(a)}(\mathbf{a}, \mathbf{b}) = g^{(a)}(a_k, b_k) + \sum_{j=1}^N c^{(a)}(a_j, b_j), \quad (16)$$

with $c^{(a)}$ and $g^{(a)}$ being independent on the oscillator indices k and j , respectively. A similar argument is valid for $\mathbf{f}^{(b)}$. Sorting then the oscillators in a way that synchronized oscillators W_k obtain indices $k = 1, \dots, N_{\text{sync}}$, we can conclude from Eq. (16) that each of the sub-Jacobians in Eq. (15) can again be written in block-matrix form as

$$\frac{\partial \mathbf{f}^{(p)}}{\partial \mathbf{q}} = \left(\begin{array}{c|c} g_{pq} \mathbf{1} + c_{pq} E & \dots \\ \hline R_{pq} & \dots \end{array} \right),$$

wherein for $p, q \in \{a, b\}$,

$$g_{pq} := \left. \frac{\partial g^{(p)}}{\partial q} \right|_{a_1, b_1},$$

$$c_{pq} := \left. \frac{\partial c^{(p)}}{\partial q} \right|_{a_1, b_1},$$

and $\mathbf{1}, E \in \mathbb{R}^{N_{\text{sync}} \times N_{\text{sync}}}$ denote the unit matrix and the matrix with entries all equal to unity. Furthermore, the entries of $R_{pq} \in \mathbb{R}^{N_{\text{inc}} \times N_{\text{sync}}}$ are row-wise constant. From this structure, we can deduce that for perturbations affecting only the relative position of synchronized oscillators, i.e.,

$$\delta \mathbf{x}_{\perp} := (\delta a_1, \dots, \delta a_{N_{\text{sync}}}, 0, \dots, 0, \dots, \delta b_1, \dots, \delta b_{N_{\text{sync}}}, 0, \dots, 0)^T, \quad (17)$$

with

$$\sum_{k=1}^{N_{\text{sync}}} \delta a_k = \sum_{k=1}^{N_{\text{sync}}} \delta b_k = 0, \quad (18)$$

we have

$$\sum_{k=1}^{N_{\text{sync}}} d(\delta a_k)/dt = \sum_{k=1}^{N_{\text{sync}}} d(\delta b_k)/dt = 0,$$

as well as

$$d(\delta a_k)/dt = d(\delta b_k)/dt = 0$$

for $k = N_{\text{sync}} + 1, \dots, N$. Perturbations of type (17) subject to constraint (18) thus form an invariant subspace under time

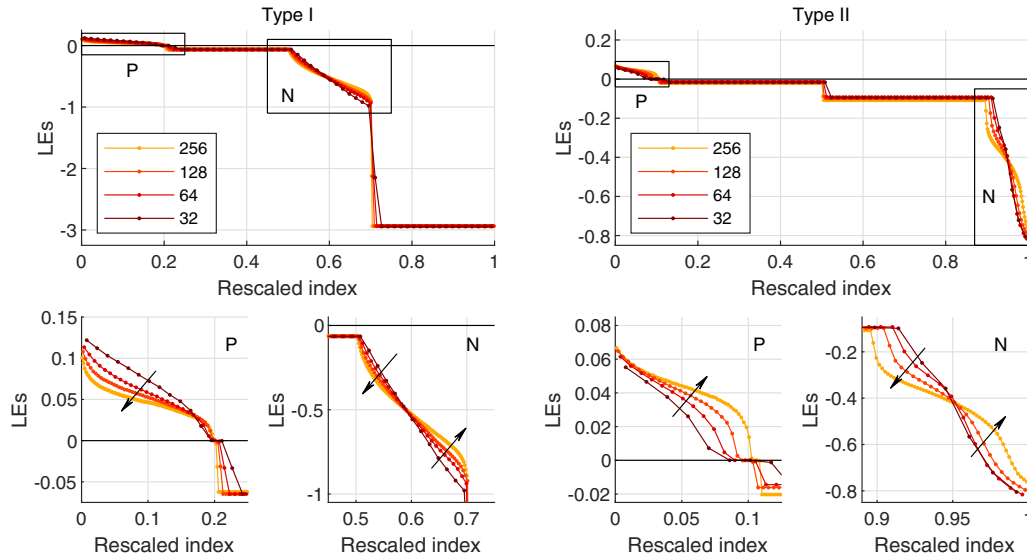


FIG. 3. Lyapunov spectra of type I and type II chimera states for increasing ensemble sizes from $N = 32$ to $N = 256$.

evolution in tangent space, the dimension of which is $2N_{\text{sync}} - 2$. Reducing tangent space dynamics to only this subspace, it is possible to obtain a two-dimensional system of linear equations, whose temporal asymptotics exactly reproduce the values of the two degenerate LEs, as obtained from the full system dynamics. Similar sets of exponents have also been found by Ku *et al.* [50] in the context of pure cluster states in oscillatory systems with linear global coupling and were termed cluster integrity exponents. Due to the very similar role of the degenerate exponents in our context, we adopt this nomenclature here, leading to the group annotations CI_1 and CI_2 .

What remains in both spectra is a small number of singleton exponents— S_1 and S_2 in the type I spectrum and only S_1 for type II—the role of which will become clear when investigating the localization properties of the associated covariant Lyapunov vectors.

B. Lyapunov spectra for larger systems

Figure 3 shows Lyapunov spectra for type I and type II chimera states in Eqs. (1) and (2). Again, the spectra are plotted against the rescaled index and include the degenerate exponents. Apart from small fluctuations of the order of two to four oscillators, the number N_{inc} of incoherent oscillators scales roughly linearly with ensemble size, so that the structure of the spectra is similar to those in Fig. 2. In particular, we find that in most cases the number of P and N exponents equals $N_{\text{inc}} - 1$ each and thus scales extensively with system size. Only for the type I spectra with $N = 128$ and $N = 256$ oscillators, there are $N_{\text{inc}} - 2$ positive exponents and one additional singleton exponent very close to zero. This, however, is likely to be an artifact. On the one hand, especially for high-dimensional systems, it may take a long time for the smallest exponents to converge properly, since these correspond naturally to the slowest directions of perturbation. On the other hand, the QR -based method for computing LEs is known to be vulnerable to numerical errors in computing close-to-zero exponents and associated BOLVs [2,51,52].

Similarly to P and N exponents, the groups of degenerate exponents scale extensively with system size, as well. In agreement with theory, we find a degeneracy of degree $N_{\text{sync}} - 1$ for each of the exponents.

While the values λ_l of the degenerate exponents do not appear to follow an obvious trend as a function of system size, the P and N exponents exhibit a pronounced size dependence with a significant trend. To give a better overview on the size dependence of the nondegenerate P and N exponents, the smaller subfigures in Fig. 3 depict magnified views onto the relevant regions. For the type I dynamics, we observe a decreasing trend for the main part of the positive exponents while some of the positive exponents close to the zero group appear to follow an increasing trend. The bulk of P group thus seems to approach a constant value, which is consistent with former results by Takeuchi *et al.* [9]. However, for the most positive exponents, the rate of decrease is slower compared to bulk and furthermore appears to slow down with increasing N . Similarly to the observations of Takeuchi *et al.*, this might indicate a subpartitioning of the positive exponents into an extensively scaling and a subextensive group.

In contrast to the type I case, we observe an increasing trend for the main part of the positive exponents within the type II spectra. Only some of the smallest positive exponents do not follow the increase. In particular, the smallest positive exponent seems to approach zero, so that for $N = 256$ oscillators four instead of three exponents are very close to zero. From a numerical perspective, the values of the Z-group exponents of the type II dynamics fluctuate stronger compared to the those of the type I spectra. This might indicate difficulties with the numerical integration method. Still, it might also give an indication that in the limit of large system sizes some of the CLVs come very close to those of the zero subspace and should thus be explored further.

The N group of negative exponents appears to flatten with increasing system size for both types of chimera states, i.e., more negative exponents increase, whereas less negative exponents decrease. For the type I spectra, this results in an increasingly tangential shape of the spectral curve. A similar

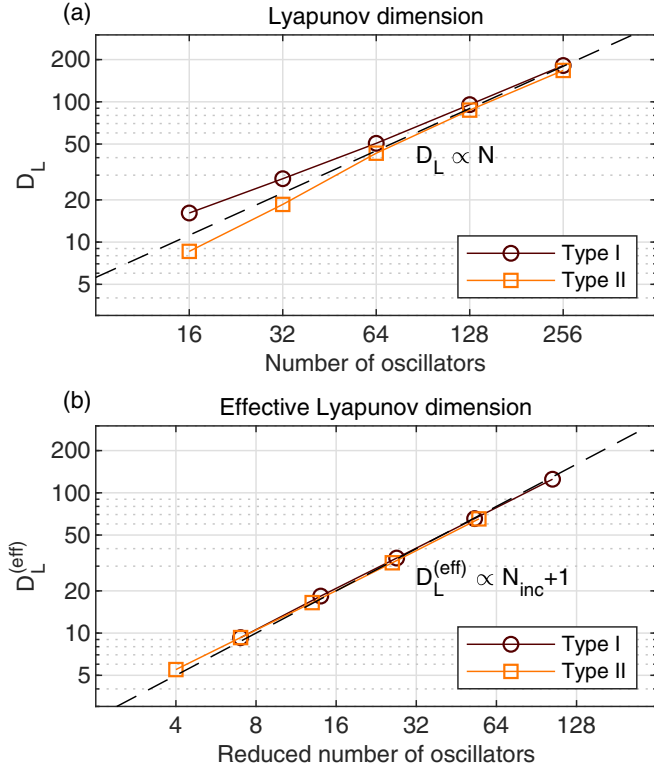


FIG. 4. (a) Lyapunov dimensions type I and a type II chimera states as a function of N . (b) Effective Lyapunov dimension as a function of the reduced number of oscillators $N_{inc} + 1$.

pattern is found also within the type II spectra. A difference, however, occurs in the behavior of the most negative exponents between $\tilde{l} = 0.95$ and $\tilde{l} = 1$. Within this range, the type II spectra deviate significantly from the tangentlike shape. The presence of an additional turning point in the spectral curve around $\tilde{l} = 0.975$ results in an steplike shape of the N -group spectrum and might suggest that there exist additional substructures in the spectrum, which are not resolved by the grouping structure proposed in this paper.

C. Lyapunov dimension and extensivity of type I and type II chimera states

Given the Lyapunov spectra, it is straightforward to compute also the Lyapunov dimension as stated in Eq. (8). The computed values are shown in Fig. 4(a) and reveal a monotonic increase of D_L with system size. Interestingly, the trend of the type I chimera state (at least for system sizes below $N = 256$) is not perfectly linear, but slightly slower. Going to larger system sizes, however, the deviation from linear growth decreases, suggesting that the attractor dimension of the chimera state behaves extensively in the limit $N \rightarrow \infty$. Similarly, the Lyapunov dimension appears to grow slightly faster than linear for type II chimera states, but growth slows down when considering larger systems.

The extensive nature of the attractor dimension is further strengthened by another consideration. Due to identical synchronization of $N_{sync} = N - N_{inc}$ oscillators, the system state $\hat{x}(t)$ is necessarily confined to a $2(N_{inc} + 1)$ -dimensional subspace of the $2N$ -dimensional phase space. From Eqs. (1) and

(2), it is easy to see that oscillators remain synchronized for all time, once they move in synchrony, so that this subspace is invariant under the dynamical flow. Although simulations achieve synchronization only within numerical accuracy, it thus seems natural to compute the Lyapunov dimension in a way that excludes directions orthogonal to the synchronization manifold. In Sec. IV A, we have seen that these directions correspond to the cluster integrity exponents CI_1 and CI_2 . Therefore, removing the $2(N_{sync} - 1)$ degenerate exponents before computing D_L results in an effective value of the Lyapunov dimension, $D_L^{(eff)}$, which respects the synchronization pattern. This procedure is equivalent to considering an $(N_{inc} + 1)$ -oscillator system, in which the synchronized oscillators are replaced by a single representative and weighted accordingly before taking averages. When plotting this effective dimension as a function of the reduced system size $(N_{inc} + 1)$, finite-size effects are minimized and the deviations from linear growth are marginal, as shown in Fig. 4(b). To quantify the deviation, we presumed a power-law dependence of the form

$$D_L^{(eff)} = \alpha(N_{inc} + 1)^\beta,$$

and obtained power-law exponents $\beta = 0.96$ for the type I chimera and $\beta = 0.94$ for the type II chimera from a log-log linear fit to the data. Within numerical accuracy, both exponents are well consistent with an extensive scaling of the effective Lyapunov dimension, and thus with extensively chaotic motion of the incoherent oscillators.

D. Localization of covariant Lyapunov vectors

As a last part of the Lyapunov analysis of type I and type II chimera states, we discuss the localization properties of the CLVs. Let us first focus on the CLVs corresponding to the largest Lyapunov exponents in ensembles of 128 oscillators. Figure 5 displays distributions of the magnitude of the components of a typical leading CLV for type I and type II chimeras. To begin with, it is striking that each distribution features one bin with a much larger count than all the other magnitude intervals. This peak arises from the contributions from the synchronous group which are all identical. Since the synchronized groups are larger than the incoherent ones, more than half of the entries of CLVs contribute to those magnitude bins. Furthermore, the two distributions exhibit a marked difference: While in the case of type I chimeras the magnitudes of the entries from the synchronized and incoherent oscillators are similar, there is a magnitude gap in the case of type II chimeras, the perturbation acting on the synchronous oscillators being considerably lower than the perturbations acting on the incoherent ones. This suggests that at least for this particular instant in time the perturbations remain localized within the incoherent group in case of type II chimeras, whereas type I chimeras exhibit some degree of intergroup delocalization.

Since the entries of the CLVs strongly fluctuate in time any further analysis of the existence of collective modes requires a temporal statistics of appropriate measures. Therefore we look next at the temporal distributions of the IPR as defined in Eq. (10). They are displayed for the two types of chimera states as blue (dark gray) histograms in Fig. 6. Clearly, their shapes differ drastically: The distribution from the type I dy-

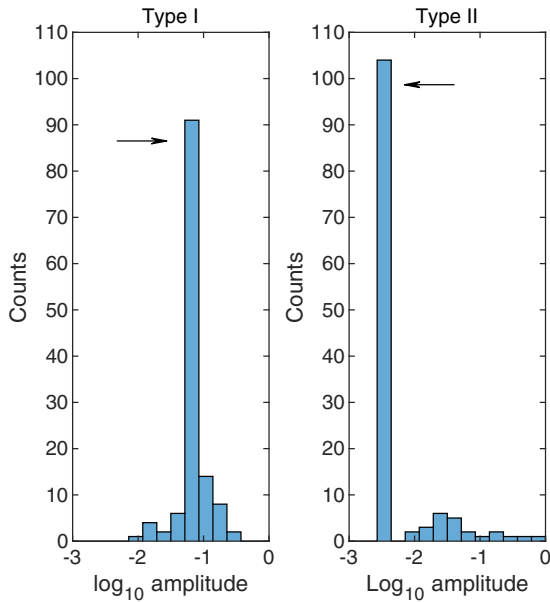


FIG. 5. Distribution of the magnitude of the entries of the leading CVL at an arbitrary instant in time for type I and type II chimeras in systems of 128 oscillators. The large peaks marked by arrows correspond to magnitude intervals which contain the magnitude entries of the synchronized oscillators.

namics is skewed with the tail toward large IPR values while the much more compact distribution of the type II chimera has a tail toward lower values of IPR and is shifted altogether to larger values. The more compact shape at larger IPR values points to a larger degree of localization of the CLVs in type II chimeras than in type I chimeras. This conjecture is backed up below by the trend of the median IPR with ensemble size.

But before we further discuss the delocalization of the CLVs within the entire ensemble, it is worthwhile to first concentrate on the intergroup delocalization of the perturbations of the first CVL. The localization indices for the synchronized and incoherent groups, ρ_{sync} and ρ_{inc} , respectively [see Eq. (11)], are depicted in Fig. 7 versus time for both chimera states. In the case of type I chimeras, the localization index of the synchronized group, although being for nearly all times smaller 1, varies largely in time and becomes equal to 1 once in a while. An index of 1 indicates that the perturbations are

spread equally across all oscillators, evidencing a “perfect” intergroup delocalization. In contrast, ρ_{sync} of the type II chimeras is always negligible, revealing that here the perturbations only affect the oscillators of the incoherent group. Note that this does not mean that the perturbations are delocalized within the incoherent group. Whether the perturbations are delocalized across many oscillators or affect only a few individual ones can only be judged from the dependence of the mean or median IPR on the ensemble size N .

It is also instructive to calculate the IPRs for the incoherent group alone (after normalizing the corresponding vectors to 1). In Fig. 6 the resulting temporal distributions are overlaid in orange (light gray) to the entire ensemble contributions. In case of the type I dynamics, the IPR distributions of the entire ensemble and of the incoherent group differ markedly. The mode of this distribution obtained without the synchronous group is shifted to the right and, more importantly, the flank to smaller IPR values is steeper, as one would expect it for an intergroup spreading of perturbations. Opposed to this, the histograms with and without synchronous group of the type II dynamics are nearly superimposable, evidencing that the contribution of the synchronous group to the IPR is negligible.

As emphasized above, the dynamics of the incoherent oscillators of the type I dynamics projected to the complex plane appears to be very similar to the stringlike chaotic dynamics in the same set of equations as studied by Nakagawa and Kuramoto [12] and Takeuchi *et al.* [8]. For easy comparison of the temporal IPR distribution of our type I chimera state with the one of collective stringlike chaos we plot the histogram of the incoherent group in a log-log-plot in Fig. 6(c) as it was done in Fig. 3(c) in Ref. [8]. The close resemblance of both IPR distributions suggests that the intragroup collective behavior corresponding to the fastest mode of the incoherent chimera group is very similar to the corresponding collective behavior in the stringlike chaotic state. In their study, Takeuchi *et al.* could go one step further and investigate the scaling of the mean IPR with the ensemble size and found that it scales with N^{-1} . Evidence of the same scaling would underline the close relation between both incoherent dynamics. However, the ensemble sizes we could computationally handle were still too small to allow for the determination of scaling properties. This task is left for future studies.

Above we discussed that the form of the distributions of the IPRs of type I and II chimeras pointed to a considerable

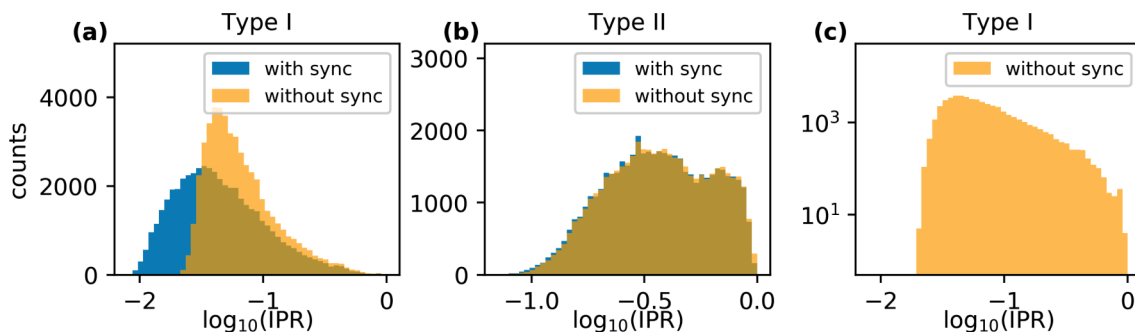


FIG. 6. Temporal distributions of the IPRs for type I [(a) and (c)] and type II (b) chimeras of the 128 oscillator ensembles. The blue (dark gray) IPR distributions were from all entries of the CLV, the orange (light gray) ones from the entries corresponding to the incoherent oscillators only (which were normalized to 1 before calculating the IPRs).

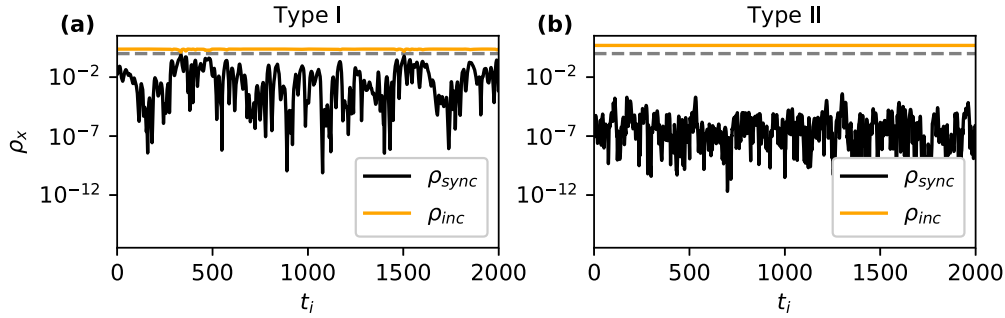


FIG. 7. Localization indices for synchronized and incoherent groups as defined in Eq. (11) for type I and type II chimeras of the 128 oscillator ensembles.

delocalization of the perturbations in case of type I but not in case of type II chimeras. This conjecture can be substantiated if we consider in analogy to Takeuchi *et al.* [8] the median of the temporal distribution as a function of the ensemble size. (Note that in Ref. [8] the mean value was taken while we consider for our asymmetric contribution the median the more appropriate choice.) A decrease of the median IPR indicates delocalization of the mode, while a value that is rather insensitive to the ensemble size N indicates localization of the perturbation. Moreover, as shown in Fig. 8 where the temporal median IPR of the CLVs is plotted as a function of the corresponding LEs, the behavior of the median IPR with system size gives concise information about the delocalization properties of all relevant CLVs. Note, however, that special care had to be taken for the cluster integrity exponents CI_1 and CI_2 , as well as for the zero exponents Z . Since all of the CLVs associated with a degenerate exponent share the same invariant subspace in tangent space, and due to linearity of the tangent space dynamics, any linear combination of two or more CLVs is again a valid CLV with the same exponent. The IPR, however, is intrinsically nonlinear and varies strongly when performing linear combinations, so that strictly speaking the IPR cannot be properly defined in degenerate subspaces. For reasons of clarity, we thus excluded the groups CI_1 and CI_2 from the plots. For the zero exponents, especially for the type II chimera state, we observed a similar effect. Knowing analytical solutions of the corresponding covariant Lyapunov vectors, however, we chose one vector to be equal to the time derivative of the dynamics $\delta\mathbf{x}_{ts}$, another one to equal the phase-shift direction $\delta\mathbf{x}_{ps}$, and the remaining one to lie within the zero-subspace, linearly independent of the former ones.

From the localization spectra, we recognize that the grouping of the Lyapunov spectra manifests itself also in the localization properties of the CLVs. Regarding the type I spectra in Fig. 8, we observe a notable decrease of the IPR with increasing system size for the largest few exponents, for close-to-zero exponents and for some of the smallest exponents. These findings are again consistent with the results of Takeuchi *et al.* [8,9], who identified five collective Lyapunov modes in similar positions for stringlike chaotic states in the same set of equations. Trivially, the zero exponents, resulting from time- and phase-shift symmetries, are associated with delocalized vectors, yielding two neutrally stable collective Lyapunov modes. Close to zero, however, we observe additional Lyapunov modes that appear to become increasingly delocalized with increasing system size and correspond to both positive and negative near-zero exponents. On the negative side, we observed already in Fig. 2 the close-to-zero singleton exponent S_1 , which possesses analogs also in spectra for larger system sizes, as visible in Fig. 3 (Type I, P). The exceptional position of this exponent in the spectra might indicate correspondence to some collective Lyapunov mode or to an otherwise special direction in phase space yet to be identified. Similarly, we observe also a small number of positive exponents, for which the median IPR appears to decrease with increasing N . However, these close-to-zero modes are hard to separate from the zero-subspace because of both, strong finite-size effects, which were also found by Takeuchi *et al.* [8], and the before-mentioned inherent numerical inaccuracies of close-to-zero exponents and associated BOLVs from QR decomposition. We thus leave the study of larger systems, which exceed our current computational facilities, for future research. Nevertheless, the qualitatively similar pattern of

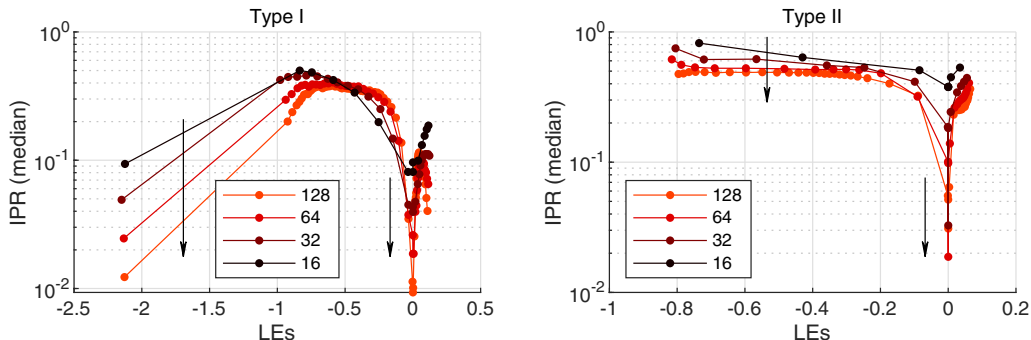


FIG. 8. Median localization of covariant Lyapunov vectors.

Lyapunov spectra and median respectively mean IPRs of the incoherent group of type I chimera states and stringlike chaos in ensembles of SL oscillators with linear global coupling reveals that the synchronized group plays only an inferior role for the macroscopic chaotic motion of the ensemble although the delocalization might spread also across the synchronized oscillators, as discussed above for the fastest collective mode. Looking at the spectrum of the type II chimera state the picture is again qualitatively different from the one of type I chimera states: a notable decrease of the median IPR is visible only for zero exponents and the ones close-by, cf. Fig. 8 (Type II). In particular, we note that in the type II spectrum neither the most positive LE nor the singleton exponent S_1 appear to be associated with a collective Lyapunov mode since their median IPR decrease only slightly with N . This substantiates that there are significant differences between the collective properties of type I and type II chimera states. It is tempting to conclude that it is the additional constraint on the dynamics of type II chimeras, the conservation of the mean oscillation (13), that impedes the formation of fast collective motion. However, at the current state of analysis this remains a hypothesis. A starting point for further investigations are type-I-like chimera states which transiently form also in Stuart-Landau ensembles subject to nonlinear global coupling [29]. If for some parameter values these states can be stabilized or at least pushed to a “supertransient regime,” a Lyapunov analysis should reveal whether also then the collective modes are suppressed or whether the stringlike chaos of the incoherent group is a signature of its collective dynamics.

V. CONCLUSION

In the present paper, we have investigated Lyapunov spectra and localization properties of the associated CLVs for two examples of chimera states in systems of globally coupled amplitude oscillators. We found that for both type I and type II chimera states the Lyapunov exponents can be subdivided into four main clusters, containing extensively many LEs, and a small number of singleton and zero exponents. Two of the main clusters, CI_1 and CI_2 , are found to consist of degenerate exponents, which are a result of the synchronization pattern of the chimera state. The corresponding perturbations affect the synchronized oscillators only, leading to the name cluster integrity exponents. A further group contains the positive exponents and indicates the hyperchaotic nature of the chimera states. For both type I and type II chimeras, the spectra exhibit a pronounced dependence on system size. While, for the type I dynamics, most of the positive LEs decrease with increasing system size toward a limiting value, the main part of the positive exponents grows to a limiting value in the case of

type II dynamics. The origin of this difference in behavior has to be addressed in future research.

Notwithstanding the different trend of the positive LEs of our two types of chimera states, the Lyapunov dimension of both dynamics grows extensively with system size. Next to the standard Lyapunov dimension, computed from the whole spectrum of LEs, we defined an effective Lyapunov dimension by neglecting the cluster integrity exponents, which measures the dimensionality only of the effective dynamics and takes account for the synchronization pattern. The size dependence of the effective Lyapunov dimension can be fitted with a power law, and yields a power-law exponent very close to unity for both type I and type II dynamics.

An analysis of the localization properties of covariant Lyapunov vectors for type I and type II chimera states revealed further differences between the dynamics. While we found evidence for at least four collective Lyapunov modes being present in the type I dynamics, two of them being associated with large positive and negative LEs, the data suggest that no more than four weak collective modes with LEs zero or close to zero exist in the type II chimera state. Furthermore, in type I chimeras the fastest collective mode spreads across both synchronous and incoherent group. Future research should set in at this point and provide additional data for larger system sizes to exclude finite-size effects from the localization spectra and to determine the exact number of collective Lyapunov modes for both types of chimera state. Here it would be of particular interest whether the collective modes form a subextensive group that grows approximately as $\mathcal{O}[\ln(N)]$ as found for stringlike chaos [9].

From a theoretical point of view, it can be expected that constraints on the system dynamics have a qualitative impact on tangent-space geometry. It therefore appears promising to investigate the geometric relation between the collective Lyapunov modes, for example in terms of angles or correlations between the vectors. Such a study could reveal information on the effective degrees of freedom within the ensemble, and might thus guide a way toward a statistical description of nonlinear amplitude oscillators subject to global coupling and constraints. To address this topic, it furthermore appears reasonable to examine in which way the collective modes affect the oscillator distribution in the complex plane. Solutions to these problems, however, have to be based on a thorough statistical analysis of the dynamics and thus require the study of oscillatory ensembles of much larger size.

ACKNOWLEDGMENTS

The authors thank S. W. Haugland for fruitful discussions. The project was funded by the Deutsche Forschungsgemeinschaft (DFG, German Research Foundation) Project No. KR1189/18.

- [1] V. Oseledets, *Trans. Mosc. Math. Soc.* **19**, 197 (1968).
 [2] A. Pikovsky and A. Politi, *Lyapunov Exponents—A Tool to Explore Complex Dynamics* (Cambridge University Press, Cambridge, 2016).

- [3] P. C. Matthews, R. E. Mirollo, and S. H. Strogatz, *Physica D* **52**, 293 (1991).
 [4] V. Hakim and W.-J. Rappel, *Phys. Rev. A* **46**, R7347(R) (1992).

- [5] N. Nakagawa and Y. Kuramoto, *Prog. Theor. Phys.* **89**, 313 (1993).
- [6] R. Livi, A. Politi, and S. Ruffo, *J. Phys. A* **19**, 2033 (1986).
- [7] T. Shibata and K. Kaneko, *Phys. Rev. Lett.* **81**, 4116 (1998).
- [8] K. A. Takeuchi, F. Ginelli, and H. Chaté, *Phys. Rev. Lett.* **103**, 154103 (2009).
- [9] K. A. Takeuchi and H. Chaté, *J. Phys. A* **46**, 254007 (2013).
- [10] F. Ginelli, P. Poggi, A. Turchi, H. Chaté, R. Livi, and A. Politi, *Phys. Rev. Lett.* **99**, 130601 (2007).
- [11] C. L. Wolfe and R. M. Samelson, *Tellus, Ser. A* **59**, 355 (2007).
- [12] N. Nakagawa and Y. Kuramoto, *Physica D* **75**, 74 (1994).
- [13] N. Nakagawa and Y. Kuramoto, *Physica D* **80**, 307 (1995).
- [14] P. V. Kuptsov and A. V. Kuptsova, *Phys. Rev. E* **90**, 032901 (2014).
- [15] M. Xu and M. R. Paul, *Phys. Rev. E* **97**, 032216 (2018).
- [16] O. E. Omel'chenko, Y. L. Maistrenko, and P. A. Tass, *Phys. Rev. Lett.* **100**, 044105 (2008).
- [17] H. Sakaguchi, *Phys. Rev. E* **73**, 031907 (2006).
- [18] D. Barkley and L. S. Tuckerman, *Phys. Rev. Lett.* **94**, 014502 (2005).
- [19] M. Wolfrum, O. E. Omel'chenko, S. Yanchuk, and Y. L. Maistrenko, *Chaos* **21**, 013112 (2011).
- [20] M. Wolfrum and O. E. Omel'chenko, *Phys. Rev. E* **84**, 015201(R) (2011).
- [21] A. E. Botha, *Sci. Rep.* **6**, 29213 (2016).
- [22] A. E. Botha and M. R. Kolahchi, *Sci. Rep.* **8**, 1830 (2018).
- [23] L. Schmidt, K. Schönleber, K. Krischer, and V. García-Morales, *Chaos* **24**, 013102 (2014).
- [24] K. Schönleber, C. Zensen, A. Heinrich, and K. Krischer, *New J. Phys.* **16**, 063024 (2014).
- [25] M. J. Panaggio and D. M. Abrams, *Nonlinearity* **28**, R67 (2015).
- [26] F. P. Kemeth, S. W. Haugland, L. Schmidt, I. G. Kevrekidis, and K. Krischer, *Chaos* **26**, 094815 (2016).
- [27] E. Schöll, *Eur. Phys. J. Special Top.* **225**, 891 (2016).
- [28] O. E. Omel'chenko, *Nonlinearity* **31**, R121 (2018).
- [29] L. Schmidt and K. Krischer, *Chaos* **25**, 064401 (2015).
- [30] G. C. Sethia and A. Sen, *Phys. Rev. Lett.* **112**, 144101 (2014).
- [31] J. Thompson and H. B. Stewart, *Phys. Lett. A* **103**, 229 (1984).
- [32] P. V. Kuptsov and U. Parlitz, *J. Nonlinear Sci.* **22**, 727 (2012).
- [33] F. Ginelli, H. Chaté, R. Livi, and A. Politi, *J. Phys. A* **46**, 254005 (2013).
- [34] H. Bosetti and H. A. Posch, *Chem. Phys.* **375**, 296 (2010).
- [35] D. P. Truant and G. P. Morriss, *Phys. Rev. E* **90**, 052907 (2014).
- [36] H.-I. Yang and G. Radons, *J. Phys. A* **46**, 254015 (2013).
- [37] M. Xu and M. R. Paul, *Phys. Rev. E* **93**, 062208 (2016).
- [38] S. Vannitsem and V. Lucarini, *J. Phys. A* **49**, 224001 (2016).
- [39] K. A. Takeuchi, H. Chaté, F. Ginelli, A. Politi, and A. Torcini, *Phys. Rev. Lett.* **107**, 124101 (2011).
- [40] J. L. Kaplan and J. A. Yorke, in *Functional Differential Equations and Approximation of Fixed Points*, Lecture Notes in Mathematics, edited by H.-O. Peitgen and H.-O. Walther (Springer, Berlin, 1979), Vol. 730, pp. 204–227.
- [41] A. Rényi, *Probability Theory* (North-Holland, Amsterdam, 1970).
- [42] P. Grassberger, *Phys. Lett. A* **97**, 227 (1983).
- [43] E. Ott, *Chaos in Dynamical Systems*, reprinted with corr ed. (Cambridge University Press, Cambridge, 1997).
- [44] A. Mirlin, *Phys. Rep.* **326**, 259 (2000).
- [45] J. R. Dormand and P. J. Prince, *J. Comput. Appl. Math.* **6**, 19 (1980).
- [46] L. F. Shampine and M. W. Reichelt, *SIAM J. Sci. Comput.* **18**, 1 (1997).
- [47] I. Shimada and T. Nagashima, *Prog. Theor. Phys.* **61**, 1605 (1979).
- [48] G. Benettin, L. Galgani, A. Giorgilli, and J.-M. Strelcyn, *Meccanica* **15**, 9 (1980).
- [49] J.-P. Eckmann and D. Ruelle, *Rev. Mod. Phys.* **57**, 617 (1985).
- [50] W. L. Ku, M. Girvan, and E. Ott, *Chaos* **25**, 123122 (2015).
- [51] L. Dieci, R. D. Russell, and E. S. van Vleck, *SIAM J. Numer. Anal.* **34**, 402 (1997).
- [52] L. Dieci and E. S. van Vleck, *Numer. Math.* **101**, 619 (2005).